

RESEARCH ARTICLE | SEPTEMBER 01 2023

Nonadiabatic dynamics near metal surfaces under Floquet engineering: Floquet electronic friction vs Floquet surface hopping

Yu Wang   ; Wenjie Dou  



J. Chem. Phys. 159, 094103 (2023)

<https://doi.org/10.1063/5.0161292>



View
Online



Export
Citation

CrossMark

Articles You May Be Interested In

Completing the dark matter solutions in degenerate Kaluza-Klein theory

J. Math. Phys. (April 2019)

Gibbs measures based on 1d (an)harmonic oscillators as mean-field limits

J. Math. Phys. (April 2018)

An upper diameter bound for compact Ricci solitons with application to the Hitchin–Thorpe inequality. II

J. Math. Phys. (April 2018)

Webinar

Boost Your Signal-to-Noise
Ratio with Lock-in Detection



Sep. 7th – Register now



Zurich
Instruments

Nonadiabatic dynamics near metal surfaces under Floquet engineering: Floquet electronic friction vs Floquet surface hopping

Cite as: J. Chem. Phys. 159, 094103 (2023); doi: 10.1063/5.0161292

Submitted: 9 June 2023 • Accepted: 10 August 2023 •

Published Online: 1 September 2023



View Online



Export Citation



CrossMark

Yu Wang^{1,2,a)}  and Wenjie Dou^{1,2,3,a)} 

AFFILIATIONS

¹ Department of Chemistry, School of Science, Westlake University, Hangzhou 310024, Zhejiang, China

² Institute of Natural Sciences, Westlake Institute for Advanced Study, Hangzhou 310024, Zhejiang, China

³ Department of Physics, School of Science, Westlake University, Hangzhou 310024, Zhejiang, China

^{a)} Authors to whom correspondence should be addressed: wangyu19@westlake.edu.cn and douwenjie@westlake.edu.cn

ABSTRACT

In the previous study Wang and Dou [J. Chem. Phys. **158**, 224109 (2023)], we have derived a Floquet classical master equation (FCME) to treat nonadiabatic dynamics near metal surfaces under Floquet engineering. We have also proposed a trajectory surface hopping algorithm to solve the FCME. In this study, we map the FCME into a Floquet Fokker–Planck equation in the limit of fast Floquet driving and fast electron motion as compared to nuclear motion. The Fokker–Planck equation is then being solved using Langevin dynamics with explicit friction and random force from the nonadiabatic effects of hybridized electrons and Floquet states. We benchmark the Floquet electronic friction dynamics against Floquet quantum master equation and Floquet surface hopping. We find that Floquet driving results in a violation of the second fluctuation–dissipation theorem, which further gives rise to heating effects.

Published under an exclusive license by AIP Publishing. <https://doi.org/10.1063/5.0161292>

I. INTRODUCTION

Floquet engineering is referred to as controlling the quantum systems with time-periodic external fields, which can give rise to various phenomena in the limit of the strong field regime.^{1,2} To model the system under Floquet engineering, we employ a periodic Hamiltonian, $H(t+T) = H(t)$. Here, T is the periodicity ($T = 2\pi/\Omega$), and Ω is the driving frequency.^{3,4} Recently, Floquet engineering is being realized by strong light–matter interactions.^{5–9} The strong light–matter interactions can result in the hybrid states, termed polaritonic states. Recent studies show that polaritons strongly modify photophysical and photochemical processes, including the enhancement of vibrational energy transfer,^{10–12} maximizing superconducting current,¹³ reducing energy losses in photovoltaics,^{14,15} tilting the ground-state reactivity landscape,^{16–18} etc.

The problem we are concerned with in this study is the Floquet engineered nonadiabatic (electron transfer and vibrational relaxation) processes at the molecule–metal interface. Actually, Floquet driving on the system can be mapped onto the case of driving on a

metal surface.^{19,20} Therefore, the methods in this study can be widely used in the plasmon-assisted chemistry,²¹ such as water splitting^{22–24} and the reduction of carbon dioxide.^{25–27} In addition, our methods can be used in the field of surface-enhanced Raman scattering (SERS) for biological and chemical sensing applications.^{28,29} In our previous work,³⁰ we have derived a Floquet classical master equation (FCME) to describe Floquet engineered nonadiabatic dynamics near metal surfaces. We have also proposed a Floquet surface hopping (FSH) algorithm to solve the FCME, where we evolve trajectories on the potential energy surfaces (PESs) with stochastic hopping between different PESs. The hopping rates are determined by the Floquet replicas modified molecule–metal interactions. This method is valid when two conditions are met: (1) high temperature limit ($\hbar\omega \ll kT$) so that the nuclear motion can be treated classically; and (2) weak molecule–metal coupling ($\Gamma \ll kT$) so that the effect of molecular level broadening can be disregarded. We have also benchmarked our FSH algorithm, where FSH agrees with the FQME well as long as the nuclei can be treated classically regardless of the driving amplitude and driving frequency. Note that the

advantage of the FCME over the FQME is that the FCME can be easily applied to many nuclear degrees of freedom with anharmonic potentials.

In this paper, we show that in the limit of strong molecule–metal coupling ($\hbar\omega \ll \Gamma$) and fast Floquet driving ($\hbar\omega \ll \hbar\Omega$) as compared to nuclear motion, indeed, these regimes are very relevant to the application of plasmonic chemistry.^{24,31} The FCME can be mapped onto a Floquet Fokker–Planck (FFP) equation with Floquet replicas, modified damping force, and random force. This FFP equation can be then solved easily by Langevin dynamics with explicit Floquet electronic friction (FEF). It is known that electronic friction theory has widely been implemented in nonadiabatic processes on metal surfaces.^{32–34} Here, we benchmark the FEF against the FQME and FSH for electronic population and nuclear kinetic energy dynamics under different Floquet driving amplitudes (A) and frequencies (Ω). We find that FEF fails to capture the oscillation feature caused by Floquet driving at small driving frequencies. By contrast, FEF agrees well with the FQME and FSH under fast Floquet drivings regardless of driving amplitudes. We further observe that the violation of the second fluctuation–dissipation theorem induced by Floquet driving leads to the heating effect of nuclear motion, especially under strong driving amplitude.

The structure of this paper is organized as follows: In Sec. II, we show the derivation of the FFP equation from the FCME. In Sec. III, we benchmark the dynamics for electronic population as well as nuclear kinetic energy from the FFP equation against the FQME and FSH methods. Finally, we conclude in Sec. IV.

II. THEORY

A. Floquet classical master equation (FCME)

We start from the Anderson–Holstein (AH) model with the periodic drivings acting on the impurity energy level (molecule), which is coupled both to a vibrational degree of freedom (DoF) and a continuum of electronic states,

$$\hat{H} = \hat{H}_S + \hat{H}_B + \hat{H}_T, \quad (1)$$

$$\hat{H}_S = (E(x) + A \sin(\Omega t))d^\dagger d + V_0(x) + \frac{p^2}{2M}, \quad (2)$$

$$\hat{H}_B = \sum_k \varepsilon_k c_k^\dagger c_k, \quad (3)$$

$$\hat{H}_T = \sum_k V_k(d^\dagger c_k + c_k^\dagger d), \quad (4)$$

Here $d(d^\dagger)$ and $c_k(c_k^\dagger)$ are the annihilation (creation) operators for an electron in the impurity (subsystem) and in the continuum (bath), $E(x)$ is the on-site energy for the impurity that depends on nuclear position. $V_0(x)$ is the diabatic potential energy surface (PES) for the unoccupied state. We can further define the diabatic PES for the (time-independent) occupied state as $V_1(x) = V_0(x) + E(x)$. The periodic driving acts on the impurity energy level with a driving amplitude A and a driving frequency Ω . Without loss of generality, we assume that $V_0(x)$ is taken the form of a harmonic oscillator

$$V_0(x) = \frac{1}{2}M\omega^2 x^2. \quad (5)$$

In the FCME, we define the classical phase space probability densities $P_0(x, p, t)$ ($P_1(x, p, t)$) for the nuclear DoFs with the impurity level being unoccupied (occupied). The time evolution of phase space probability densities is given by³⁰

$$\begin{aligned} \frac{\partial P_0(x, p, t)}{\partial t} = & \frac{\partial V_0(x)}{\partial x} \frac{\partial P_0(x, p, t)}{\partial p} - \frac{p}{M} \frac{\partial P_0(x, p, t)}{\partial x} \\ & - \gamma_{0 \rightarrow 1}(t)P_0(x, p, t) + \gamma_{1 \rightarrow 0}(t)P_1(x, p, t), \end{aligned} \quad (6)$$

$$\begin{aligned} \frac{\partial P_1(x, p, t)}{\partial t} = & \frac{\partial V_1(x)}{\partial x} \frac{\partial P_1(x, p, t)}{\partial p} - \frac{p}{M} \frac{\partial P_1(x, p, t)}{\partial x} \\ & + \gamma_{0 \rightarrow 1}(t)P_0(x, p, t) - \gamma_{1 \rightarrow 0}(t)P_1(x, p, t), \end{aligned} \quad (7)$$

where

$$\gamma_{0 \rightarrow 1}(t) = \frac{\Gamma}{\hbar} \tilde{f}(E(x)), \quad (8)$$

$$\gamma_{1 \rightarrow 0}(t) = \frac{\Gamma}{\hbar} (1 - \tilde{f}(E(x))), \quad (9)$$

Here, $\tilde{f}(E(x))$ is the modified Fermi function with Floquet replicas, which is given by

$$\begin{aligned} \tilde{f}(E(x)) = & \sum_{nm} \cos\{(n-m)(\Omega t + \pi/2)\} \\ & \times J_n(z)J_m(z) \frac{1}{1 + e^{\beta(E(x) - m\Omega)}}, \end{aligned} \quad (10)$$

where n, m are integers ranging from $-\infty$ to $+\infty$. $J_n(z)$ is the n -th Bessel function of the first kind with $z = \frac{A}{\hbar\Omega}$.

In the limit of fast driving, we can perform the time average on $\tilde{f}(E(x))$, such that we arrive at a time-independent $\bar{f}(E(x))$

$$\bar{f}(E(x)) = \sum_n |J_n(z)|^2 \frac{1}{1 + e^{\beta(E(x) - n\Omega)}} \quad (11)$$

Correspondingly, time-averaged hopping rate $\bar{\gamma}_{0 \rightarrow 1}$ ($\bar{\gamma}_{1 \rightarrow 0}$) is also time-independent. Here, Γ is the hybridization function given by

$$\Gamma(\varepsilon) = 2\pi \sum_k |V_k|^2 \delta(\varepsilon_k - \varepsilon). \quad (12)$$

In the wide band limit, we can assume that Γ is a constant (i.e., does not change with ε or x). Note that the driving frequency Ω and the Γ should satisfy $\hbar\Omega, \Gamma \ll |\varepsilon_{\max} - \varepsilon_{\min}|$, where ε_{\max} and ε_{\min} are band edges of the metal surface,¹⁹ to meet the wide band approximation.

The equation of motion for the phase space densities in this FCME can be solved via a Floquet surface hopping algorithm in real time, which is denoted as the Floquet averaged surface hopping with density (FaSH-density) algorithm. In short, in the FaSH-density algorithm, we use time-averaged $\bar{\gamma}_{0 \rightarrow 1}$ ($\bar{\gamma}_{1 \rightarrow 0}$) as the hopping rates to propagate nuclear dynamics, whereas we use time-dependent hopping rate to propagate electronic dynamics via $\dot{P}_0 = -\gamma_{0 \rightarrow 1}P_0 + \gamma_{1 \rightarrow 0}P_1$ and $\dot{P}_1 = \gamma_{0 \rightarrow 1}P_0 - \gamma_{1 \rightarrow 0}P_1$. The electronic population is then calculated using P_0 and P_1 . See Ref. 30 for details. For simplicity, we use FSH to refer to FaSH-density in the following.

B. Floquet Fokker-Planck equation (FFP)

We now map the Floquet CME into a Floquet FP equation with explicit electronic friction and random force. To do so, we first define new densities $A(x, p, t)$ and $B(x, p, t)$ as (similar to Ref. 35)

$$P_0(x, p, t) = (1 - \bar{f}(E(x)))A(x, p, t) + B(x, p, t), \quad (13)$$

$$P_1(x, p, t) = \bar{f}(E(x))A(x, p, t) - B(x, p, t). \quad (14)$$

Note that $A(x, p, t) = P_0(x, p, t) + P_1(x, p, t)$, which is the total probability density. When the electronic motion and Floquet driving are very fast, the phase space densities P_0 and P_1 will be very close to equilibrium densities $(1 - \bar{f}(E(x)))A$ and $\bar{f}(E(x))A$, respectively. Such that $B(x, p, t)$ can be seen as the nonadiabatic phase space density.

The time evolution of $A(x, p, t)$ can be obtained by plugging Eqs. (13) and (14) into Eqs. (6) and (7),

$$\begin{aligned} \frac{\partial A(x, p, t)}{\partial t} = & -\frac{p}{M} \frac{\partial A(x, p, t)}{\partial x} + \left(\frac{\partial V_0(x)}{\partial x} + \frac{d(E(x))}{dx} \bar{f} \right) \\ & \times \frac{\partial A(x, p, t)}{\partial p} - \frac{d(E(x))}{dx} \frac{\partial B(x, p, t)}{\partial p} \end{aligned} \quad (15)$$

The time evolution of $B(x, p, t) = \bar{f}(E(x))P_0(x, p, t) - (1 - \bar{f}(E(x)))P_1(x, p, t)$ can be formulated as

$$\begin{aligned} \frac{\partial B(x, p, t)}{\partial t} = & -\frac{p}{M} \frac{\partial B(x, p, t)}{\partial x} + \frac{\partial V_0(x)}{\partial x} \frac{\partial B(x, p, t)}{\partial p} \\ & + \frac{p}{M} A(x, p, t) \frac{\partial \bar{f}}{\partial x} - \frac{d(E(x))}{dx} \bar{f} (1 - \bar{f}) \frac{\partial A(x, p, t)}{\partial p} \\ & + \frac{d(E(x))}{dx} (1 - \bar{f}) \frac{\partial B(x, p, t)}{\partial p} \\ & - \Gamma B(x, p, t) - \Gamma (\bar{f} - \bar{f}) A. \end{aligned} \quad (16)$$

Note that we only invoked the fast driving approximation ($\Omega > \omega$), so far, such that Eqs. (15) and (16) are exact as long as FCME is valid. We now invoke the assumption of fast electronic motion as compared to nuclear motion ($\Gamma > \hbar\omega$). In such a limit, the phase space densities are very close to equilibrium densities. Hence, $B(x, p, t)$ should be small relative to $A(x, p, t)$ and change slowly with respect to x, p , and t . Such that several terms in Eq. (16) can be ignored,

$$\begin{aligned} B(x, p, t) \approx & -\frac{d(E(x))}{dx} \frac{1}{\Gamma} \bar{f} (1 - \bar{f}) \frac{\partial A(x, p, t)}{\partial p} \\ & + \frac{p}{\Gamma M} A(x, p, t) \frac{\partial \bar{f}}{\partial x} - (\bar{f} - \bar{f}) A. \end{aligned} \quad (17)$$

If we substitute Eq. (17) back into Eq. (15), we arrive at a FFP equation with a periodic driving system,

$$\begin{aligned} \frac{\partial A(x, p, t)}{\partial t} = & -\frac{p}{M} \frac{\partial A(x, p, t)}{\partial x} + \frac{\partial U(x, t)}{\partial x} \frac{\partial A(x, p, t)}{\partial p} \\ & + \gamma_e(x) \frac{\partial}{\partial p} (pA(x, p, t)) + D(x) \frac{\partial^2 A(x, p, t)}{\partial p^2}. \end{aligned} \quad (18)$$

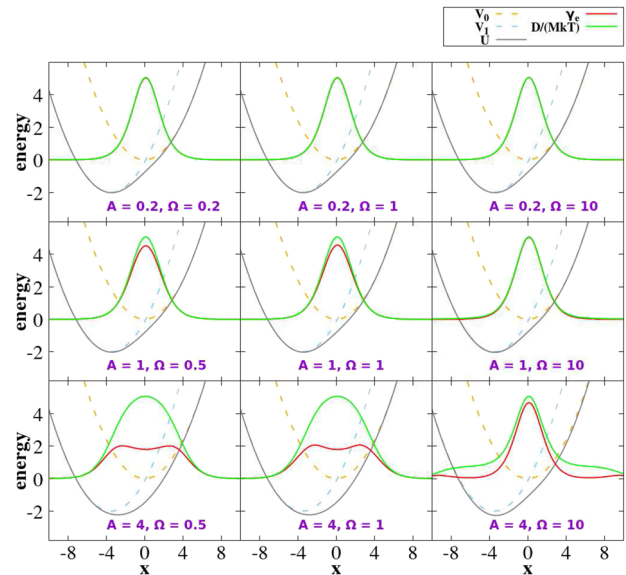


FIG. 1. Diabatic potential V_0 [Eq. (5), yellow dash line] and V_1 (blue dash line), time-averaged potential of mean force (aPMF) $U(x)$ [Eq. (23), gray solid line], electronic friction $\gamma_e(x)$ [Eq. (19), red solid line], and $\gamma'_e(x)$ [Eq. (20), green solid line] as a function of position x under different driving amplitudes A and driving frequencies Ω . $g = 0.75$, $\hbar\omega = 0.3$, $\Gamma = 1$, $\bar{E}_d = -2$, $kT = 1$.

Here, $\gamma_e(x)$ is the electronic friction coefficient,

$$\gamma_e(x) = -\frac{1}{\Gamma M} \frac{dE(x)}{dx} \frac{\partial \bar{f}}{\partial x}. \quad (19)$$

The correlation function of the random force is $D(x) = \gamma'_e(x) MkT$. We have defined $\gamma'_e(x)$ as

$$\gamma'_e(x) = \frac{\beta}{\Gamma M} \left(\frac{dE(x)}{dx} \right)^2 \bar{f} (1 - \bar{f}) \quad (20)$$

and $\frac{\partial U(x, t)}{\partial x}$ is the time-dependent mean force

$$\frac{\partial U(x, t)}{\partial x} = \hbar\omega x + \frac{d(E(x))}{dx} \bar{f}. \quad (21)$$

We can write the time-dependent potential of mean force (PMF) $U(x, t)$ explicitly as (up to a constant),

$$\begin{aligned} U(x, t) = & \frac{1}{2} \hbar\omega x^2 - \frac{1}{\beta} \sum_{nm} \cos \{ (n - m)(\Omega t + \pi/2) \} \\ & \times J_n(z) J_m(z) \log(1 + \exp(-\beta(E(x) - m\Omega))) \end{aligned} \quad (22)$$

If we further invoke the time average on the PMF, we arrive at the time-averaged PMF (aPMF) as

$$\bar{U}(x) = \frac{1}{2} M\omega x^2 - \frac{1}{\beta} \sum_n |J_n(z)|^2 \log(1 + \exp(-\beta(E(x) - n\Omega))). \quad (23)$$

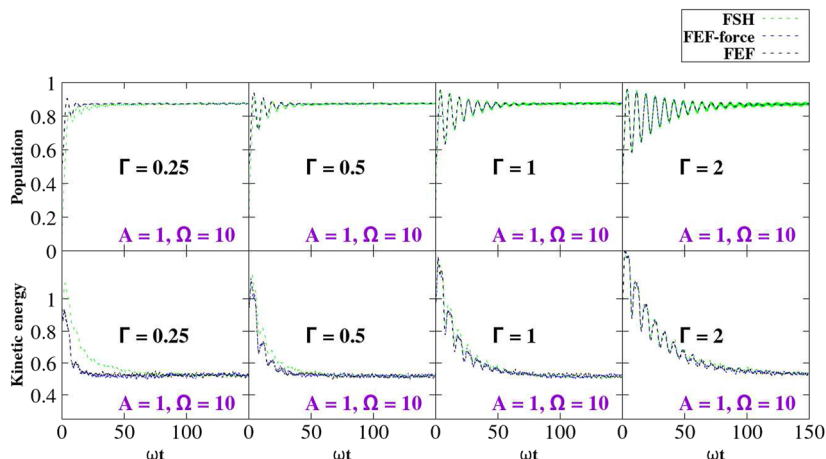


FIG. 2. Electronic population and nuclear kinetic energy as a function of time for different Γ . The driving amplitude and frequency are fixed $A = 1$ and $\Omega = 10$. We prepare an initial state satisfying the Boltzmann distribution at temperature $2T$. Note that FEF(FEF-force) agrees well with FSH in the limit of $\Gamma \gg \hbar\omega$. Parameters: $g = 0.75$, $\hbar\omega = 0.3$, $\Gamma = 1$, $\bar{E}_d = -2$, and $kT = 1$.

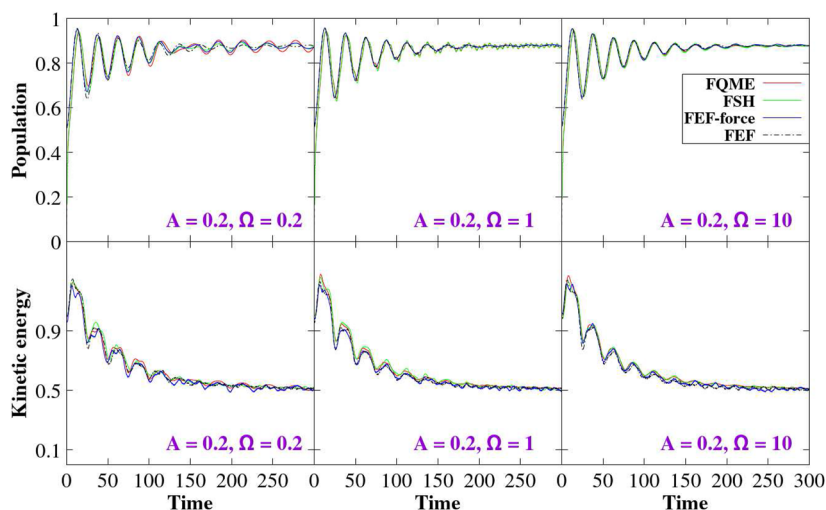


FIG. 3. Electronic population and nuclear kinetic energy as a function of time for different driving frequencies ($\Omega = 0.2, 1$, and 10) under a small driving amplitude $A = 0.2$. $g = 0.75$, $\hbar\omega = 0.3$, $\Gamma = 1$, $\bar{E}_d = -2$, and $kT = 1$. Note that the four methods (FQME, FSH, FEF-force, and FEF) give nearly the same features of dynamics under small strength of drivings.

This FFP can be solved via Floquet electronic friction-Langevin dynamics either with time-dependent potential energy surface $U(x, t)$ (FEF-force), or with time-independent $\bar{U}(x)$ (FEF)

$$\dot{p} = -\frac{\partial U}{\partial x} - \gamma_e p + \xi, \quad (24)$$

$$\dot{x} = \frac{p}{M}, \quad (25)$$

where ξ is the random force that is assumed to be a Gaussian variable with a norm $\sigma = \sqrt{2M\gamma_e kT/dt}$. Again, dt is the time step interval.

We use fourth Runge-Kutta to integrate Eqs. (24) and (25), and 10000 trajectories are used for both FSH and FEF simulations.

Equations (18)–(23) are the main results of this paper. To better understand these formulas, $E(x)$ is chosen to be a linear dependence on x ,

$$E(x) = \sqrt{2}gx + E_d. \quad (26)$$

We define the renormalized energy as $\bar{E}_d \equiv E_d - E_r$, where $E_r = g^2/\hbar\omega$ is the reorganization energy. In Fig. 1, we plot the aPMF $\bar{U}(x)$ [Eq. (23)], electronic friction $\gamma_e(x)$ [Eq. (19)], and $\gamma_e'(x)$

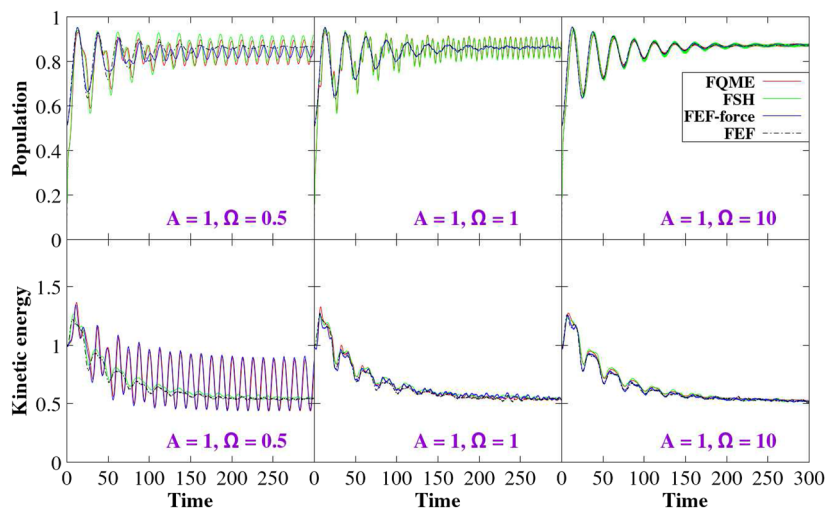


FIG. 4. Electronic population and nuclear kinetic energy as a function of time for different driving frequencies ($\Omega = 0.5, 1,$ and 10) under a medium strength of driving amplitude $A = 1$. $g = 0.75, \hbar\omega = 0.3, \Gamma = 1, \bar{E}_d = -2,$ and $kT = 1$. Note that the FEF method using time-independent aPMF fails to capture the oscillation feature introduced by the drivings at small driving frequencies ($\Omega = 0.5$ or 1).

[Eq. (20)] as a function of x under different driving conditions. It is noteworthy that when driving amplitude ($A = 1$ or 4) is much larger than nuclear oscillation ($\hbar\omega = 0.3$), $\gamma_e \neq \gamma'_e = \frac{D(x)}{MkT}$, which violates the second fluctuation–dissipation theorem. The heating effects on nuclear motion arise from such violations as seen in the Results section. The code is available online.³⁶

III. RESULTS

First, we compare the electronic and nuclear dynamics between Floquet surface hopping and Floquet electronic friction methods. In Floquet electronic friction, we could either use the time-dependent PMF (denoted as FEF-force) or the time-independent aPMF (denoted as FEF). In Fig. 2, we benchmark these Floquet electronic friction methods for different Γ . We fix the driving amplitude $A = 1$ and driving frequency $\Omega = 10$ and prepare the initial states of the oscillators in one well with a Boltzmann distribution at temperature $2T$. Similar to the non-Floquet case,³⁵ the potential of mean force is a mixture of two diabatic potentials of energy surfaces (PESs), such that the initial ($t = 0$) electronic populations from FEF are not equal to 1. In the long time dynamics of the electronic population, Floquet electronic friction agrees with Floquet surface hopping very well. As for the nuclear dynamics, when electronic motion is fast (large Γ), we reach good agreements between Floquet surface hopping and Floquet electronic friction. As expected, Floquet electronic friction fails in the slow electronic motion limit (small Γ). Below, we mainly focus on the large Γ limit.

We now benchmark the FEF and FSH against the Floquet quantum master equation (FQME). The FQME is exact as long as the broadening effects from the lead can be ignored $\Gamma < kT$. Details on FQME can be found in Ref. 30.

In Fig. 3, we benchmark the Floquet electronic friction method under relatively small driving amplitude ($A = 0.2$), which is comparable to the nuclear oscillation ($\hbar\omega = 0.3$). In such a case, all these four methods nearly agree with each other regardless of the driving frequencies. Note that under small driving frequency ($\Omega = 0.2$), electronic dynamics reach to a limit cycle, instead of a steady state, which can be reflected by the FQME, FSH, and FEF-force. The FEF method fails to reproduce this limit cycle feature since we average the time-dependent PMF. Under large driving frequency ($\Omega = 10$), the electronic populations reach a steady state of $N = \tilde{f}(\bar{E}_d)$, and nuclear kinetic energy reaches a steady state of $\frac{kT}{2}$, where T is the temperature of the metal bath.

We now turn to the case of medium strength in driving amplitude ($A = 1$), as shown in Fig. 4. The oscillation feature from the FQME, FSH, and FEF-force under small driving frequencies ($\Omega = 0.5, 1$) is more pronounced than the small driving amplitude case (Fig. 3), which reaches a cycle limit in a long time. Note that FEF-force gives smaller oscillation feature for electronic population in the limit cycle as compared to the FQME, whereas the FEF method fails to capture these oscillations. In the limit of high driving frequency ($\Omega = 10$), all these methods reach the same steady state for both electronic and nuclear dynamics.

Finally, we show the case where the driving amplitude is relatively large ($A = 4$) in Fig. 5. In this limit, the oscillation feature is very strong, especially when the driving frequency is small. Again, FEF fails to capture these oscillation features when the driving is slow. FEF-force predicts the oscillator features with a smaller oscillating amplitude. It is noteworthy that under such strong driving amplitude, the nuclear kinetic energies reach a steady state above $\frac{kT}{2}$. This violation of the second fluctuation–dissipation theorem is due to the Floquet driving, as shown in Fig. 1. Such a nonequilibrium condition gives rise to the heating effect of nuclear motion.

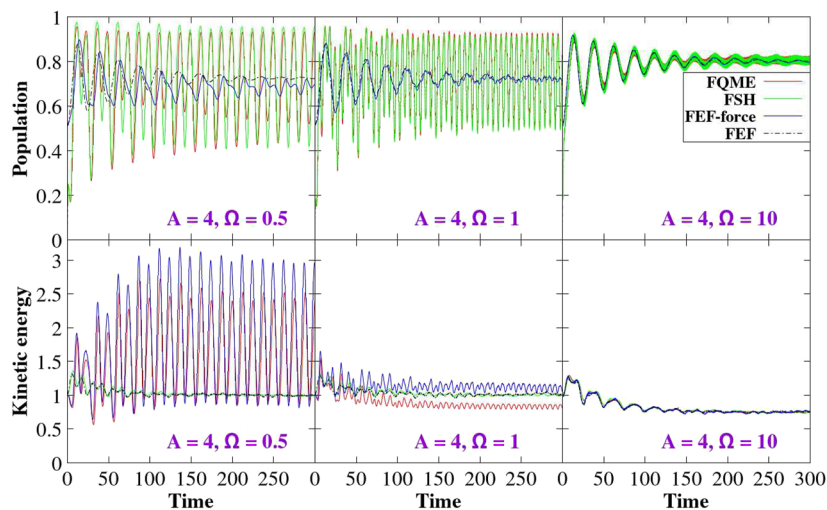


FIG. 5. Electronic population and nuclear kinetic energy as a function of time for different driving frequencies ($\Omega = 0.5, 1,$ and 10) under a strong driving amplitude $A = 4$. $g = 0.75, \hbar\omega = 0.3, \Gamma = 1, \bar{E}_d = -2,$ and $kT = 1$. FEF fails to capture the oscillation features when the driving is slow ($\Omega = 0.5$ or 1). FEF-force predicts the oscillator features with smaller oscillating amplitude. The effective temperature of nuclear motion is above $\frac{kT}{2}$, which arises from the violation of the second fluctuation–dissipation theorem.

IV. CONCLUSIONS

In this paper, we derived a Floquet Fokker–Planck equation (FFP) to characterize the Floquet classical master equation (FCME) in the limit of slow nuclear motion as compared to fast electronic motion as well as fast external driving ($\Gamma \gg \hbar\omega$ and $\hbar\Omega \gg \hbar\omega$). The FFP can be solved using Langevin dynamics with explicit Floquet replicas, modified electronic friction, and random force. By employing time-dependent and time-averaged mean force, we proposed two FEF methods in this study, which agree well with the FQME and FSH under fast Floquet drivings regardless of driving amplitudes. We find that Floquet driving leads to a violation of the second fluctuation–dissipation theorem, especially under large driving amplitudes, which gives rise to a heating effect on nuclear motion. Our method offers an alternative means to study non-adiabatic dynamics with periodic drivings in an open quantum system.

ACKNOWLEDGMENTS

This material is based on work supported by the National Natural Science Foundation of China (NSFC Grant No. 22273075). W.D. acknowledges start-up funding from Westlake University.

AUTHOR DECLARATIONS

Conflict of Interest

The authors have no conflicts to disclose.

Author Contributions

Yu Wang: Conceptualization (equal); Data curation (equal); Writing – original draft (equal). **Wenjie Dou:** Conceptualization

(equal); Funding acquisition (equal); Supervision (equal); Writing – review & editing (equal).

DATA AVAILABILITY

The data that support the findings of this study are available from the corresponding authors upon reasonable request.

REFERENCES

- T. Oka and S. Kitamura, “Floquet engineering of quantum materials,” *Annu. Rev. Condens. Matter Phys.* **10**, 387–408 (2019).
- M. A. Sentef, J. Li, F. Künzel, and M. Eckstein, “Quantum to classical crossover of Floquet engineering in correlated quantum systems,” *Phys. Rev. Res.* **2**, 033033 (2020).
- G. Engelhardt and J. Cao, “Dynamical symmetries and symmetry-protected selection rules in periodically driven quantum systems,” *Phys. Rev. Lett.* **126**, 090601 (2021).
- G. Cabra, I. Franco, and M. Galperin, “Optical properties of periodically driven open nonequilibrium quantum systems,” *J. Chem. Phys.* **152**, 094101 (2020).
- G. Günter, A. A. Anappara, J. Hees, A. Sell, G. Biasiol, L. Sorba, S. De Liberato, C. Ciuti, A. Tredicucci, A. Leitenstorfer, and R. Huber, “Sub-cycle switch-on of ultrastrong light–matter interaction,” *Nature* **458**, 178–181 (2009).
- M. Engel, M. Steiner, A. Lombardo, A. C. Ferrari, H. v. Löhneysen, P. Avouris, and R. Krupke, “Light–matter interaction in a microcavity-controlled graphene transistor,” *Nat. Commun.* **3**, 906 (2012).
- T. W. Ebbesen, “Hybrid light–matter states in a molecular and material science perspective,” *Acc. Chem. Res.* **49**, 2403–2412 (2016).
- P. Forn-Díaz, L. Lamata, E. Rico, J. Kono, and E. Solano, “Ultrastrong coupling regimes of light–matter interaction,” *Rev. Mod. Phys.* **91**, 025005 (2019).
- F. J. Garcia-Vidal, C. Ciuti, and T. W. Ebbesen, “Manipulating matter by strong coupling to vacuum fields,” *Science* **373**, eabd0336 (2021).
- D. M. Coles, N. Somaschi, P. Michetti, C. Clark, P. G. Lagoudakis, P. G. Savvidis, and D. G. Lidzey, “Polariton-mediated energy transfer between organic dyes in a strongly coupled optical microcavity,” *Nat. Mater.* **13**, 712–719 (2014).

- ¹¹K. Georgiou, P. Michetti, L. Gai, M. Cavazzini, Z. Shen, and D. G. Lidzey, "Control over energy transfer between fluorescent BODIPY dyes in a strongly coupled microcavity," *ACS Photonics* **5**, 258–266 (2018).
- ¹²B. Xiang, R. F. Ribeiro, M. Du, L. Chen, Z. Yang, J. Wang, J. Yuen-Zhou, and W. Xiong, "Intermolecular vibrational energy transfer enabled by microcavity strong light–matter coupling," *Science* **368**, 665–667 (2020).
- ¹³I. Gimeno, W. Kersten, M. C. Pallarés, P. Hermosilla, M. J. Martínez-Pérez, M. D. Jenkins, A. Angerer, C. Sánchez-Azqueta, D. Zueco, J. Majer *et al.*, "Enhanced molecular spin-photon coupling at superconducting nanoconstrictions," *ACS Nano* **14**, 8707–8715 (2020).
- ¹⁴V. C. Nikolis, A. Mischok, B. Siegmund, J. Kublitski, X. Jia, J. Benduhn, U. Hörmann, D. Neher, M. C. Gather, D. Spoltore, and K. Vandewal, "Strong light-matter coupling for reduced photon energy losses in organic photovoltaics," *Nat. Commun.* **10**, 3706 (2019).
- ¹⁵M. Wang, M. Hertzog, and K. Börjesson, "Polariton-assisted excitation energy channeling in organic heterojunctions," *Nat. Commun.* **12**, 1874 (2021).
- ¹⁶A. Thomas, L. Lethuillier-Karl, K. Nagarajan, R. M. A. Vergauwe, J. George, T. Chervy, A. Shalabney, E. Devaux, C. Genet, J. Moran, and T. W. Ebbesen, "Tilting a ground-state reactivity landscape by vibrational strong coupling," *Science* **363**, 615–619 (2019).
- ¹⁷J. Galego, C. Climent, F. J. Garcia-Vidal, and J. Feist, "Cavity casimir-polder forces and their effects in ground-state chemical reactivity," *Phys. Rev. X* **9**, 021057 (2019).
- ¹⁸J. Lather, P. Bhatt, A. Thomas, T. W. Ebbesen, and J. George, "Cavity catalysis by cooperative vibrational strong coupling of reactant and solvent molecules," *Angew. Chem., Int. Ed.* **58**, 10635–10638 (2019).
- ¹⁹M. Kuperman, L. Nagar, and U. Peskin, "Mechanical stabilization of nanoscale conductors by plasmon oscillations," *Nano Lett.* **20**, 5531–5537 (2020).
- ²⁰S. Kohler, J. Lehmann, and P. Hänggi, "Driven quantum transport on the nanoscale," *Phys. Rep.* **406**, 379–443 (2005).
- ²¹E. Cortés, R. Grzeschik, S. A. Maier, and S. Schlücker, "Experimental characterization techniques for plasmon-assisted chemistry," *Nat. Rev. Chem.* **6**, 259–274 (2022).
- ²²K. Qian, B. C. Sweeny, A. C. Johnston-Peck, W. Niu, J. O. Graham, J. S. DuChene, J. Qiu, Y.-C. Wang, M. H. Engelhard, D. Su *et al.*, "Surface plasmon-driven water reduction: Gold nanoparticle size matters," *J. Am. Chem. Soc.* **136**, 9842–9845 (2014).
- ²³P. Zhang, T. Wang, and J. Gong, "Mechanistic understanding of the plasmonic enhancement for solar water splitting," *Adv. Mater.* **27**, 5328–5342 (2015).
- ²⁴L. Yan, F. Wang, and S. Meng, "Quantum mode selectivity of plasmon-induced water splitting on gold nanoparticles," *ACS Nano* **10**, 5452–5458 (2016).
- ²⁵S. Yu, A. J. Wilson, J. Heo, and P. K. Jain, "Plasmonic control of multi-electron transfer and C–C coupling in visible-light-driven CO₂ reduction on Au nanoparticles," *Nano Lett.* **18**, 2189–2194 (2018).
- ²⁶H. Robotjazi, H. Zhao, D. F. Swearer, N. J. Hogan, L. Zhou, A. Alabastri, M. J. McClain, P. Nordlander, and N. J. Halas, "Plasmon-induced selective carbon dioxide conversion on earth-abundant aluminum-cuprous oxide antenna-reactor nanoparticles," *Nat. Commun.* **8**, 27 (2017).
- ²⁷E. B. Creel, E. R. Corson, J. Eichhorn, R. Kostecki, J. J. Urban, and B. D. McCloskey, "Directing selectivity of electrochemical carbon dioxide reduction using plasmonics," *ACS Energy Lett.* **4**, 1098–1105 (2019).
- ²⁸J. Langer, D. Jimenez de Aberasturi, J. Aizpurua, R. A. Alvarez-Puebla, B. Auguie, J. J. Baumberg, G. C. Bazan, S. E. Bell, A. Boisen, A. G. Brolo *et al.*, "Present and future of surface-enhanced Raman scattering," *ACS Nano* **14**, 28–117 (2019).
- ²⁹J. L. Payton, S. M. Morton, J. E. Moore, and L. Jensen, "A hybrid atomistic electrodynamic–quantum mechanical approach for simulating surface-enhanced Raman scattering," *Acc. Chem. Res.* **47**, 88–99 (2014).
- ³⁰Y. Wang and W. Dou, "Nonadiabatic dynamics near metal surface with periodic drivings: A Floquet surface hopping algorithm," *J. Chem. Phys.* **158**, 224109 (2023).
- ³¹K. Wu, J. Chen, J. R. McBride, and T. Lian, "Efficient hot-electron transfer by a plasmon-induced interfacial charge-transfer transition," *Science* **349**, 632–635 (2015).
- ³²C. L. Box, Y. Zhang, R. Yin, B. Jiang, and R. J. Maurer, "Determining the effect of hot electron dissipation on molecular scattering experiments at metal surfaces," *JACS Au* **1**, 164–173 (2020).
- ³³J.-T. Lü, B.-Z. Hu, P. Hedegård, and M. Brandbyge, "Semi-classical generalized Langevin equation for equilibrium and nonequilibrium molecular dynamics simulation," *Prog. Surf. Sci.* **94**, 21–40 (2019).
- ³⁴Y. Litman, E. S. Pócs, C. L. Box, R. Martinazzo, R. J. Maurer, and M. Rossi, "Dissipative tunneling rates through the incorporation of first-principles electronic friction in instanton rate theory. I. Theory," *J. Chem. Phys.* **156**, 194106 (2022).
- ³⁵W. Dou, A. Nitzan, and J. E. Subotnik, "Frictional effects near a metal surface," *J. Chem. Phys.* **143**, 054103 (2015).
- ³⁶See https://github.com/YuWANG0801/Floquet-electronic-friction/blob/main/mean_LD_friction.py for the code.